JGR Oceans

RESEARCH ARTICLE
10.1029/2019JC015825

Key Points:
- A newly established biogeochemical data set of the North Sea is used
- The variability in salinity shows distinct phase deviations from winter nutrient concentrations
- The variability of winter nutrient concentrations is mainly driven by atmospheric variability

Supporting Information:
- Supporting Information S1

Correspondence to:
J. Pätsch,
johannes.paetsch@uni-hamburg.de

Citation:
Pätsch, J., Gouretski, V., Hinrichs, I., & Koul, V. (2020). Distinct mechanisms underlying interannual to decadal variability of observed salinity and nutrient concentration in the northern North Sea. *Journal of Geophysical Research: Oceans*, *125*, e2019JC015825. https://doi.org/10.1029/2019JC015825

Received 28 OCT 2019
Accepted 28 MAR 2020
Accepted article online 4 APR 2020

Distinct Mechanisms Underlying Interannual to Decadal Variability of Observed Salinity and Nutrient Concentration in the Northern North Sea

Johannes Pätsch[1,2], Viktor Gouretski[1], Iris Hinrichs[1], and Vimal Koul[1,2]

[1]CEN (Center for Earth System Research and Sustainability), University of Hamburg, Hamburg, Germany, [2]Institute of Coastal Research, Helmholtz-Zentrum Geesthacht, Geesthacht, Germany

Abstract The influence of large-scale oceanic circulation on salinity in the northern North Sea has lead to the hypothesis that nutrient concentrations in this region are also driven by remote oceanic anomalies. Here, using a newly established biogeochemical data set of the North Sea, we show that interannual to decadal variability in winter nutrient concentrations exhibits distinct phase deviations from salinity. The variability in salinity is explained by zonal shifts in the position of the subpolar front (SPF) in the eastern North Atlantic and the associated advective delay. However, the high correlation and absence of advective delay between the position of the SPF and winter nutrient concentrations in the *Shetland region* (59–61°N, 1°W to 3°E) point to the role of atmospheric variability in driving concurrent changes in winter nutrient concentrations and the SPF position. Our analysis suggests that the prevailing wind direction and local distribution of winter nutrient concentrations together determine the interannual to decadal variability in winter nutrient concentrations in this region. In the analyzed observations, we find a strong spatial gradient in mean winter nutrient concentrations northwest of the *Shetland region*, which is absent in salinity. The horizontal shift of this spatial gradient, forced by changes in wind direction, has a larger influence on winter nutrient concentration in the *Shetland region* than the nutrient signal in oceanic anomalies originating from the eastern subpolar North Atlantic. Overall, we conclude that interannual to decadal variability in the observed nutrient concentrations is mainly driven by atmospheric variability here expressed as wind direction.

Plain Language Summary In many marine areas the winter concentration of nutrients determines the biological production of the following year. This is also true for the northern North Sea. Using a large data collection, we analyze salinity and nutrient concentrations there. We find salinity governed by the extension and retraction of a large gyre in the North Atlantic. We see consequences of the gyre dynamics 2 years later in salinity in the North Sea. Our idea was that nutrients behave similar with a time lag of 2 years. But we did not find this relation for nutrients. Instead, we find a surprising strong concurrent relation between nutrients in the North Sea and the North Atlantic gyre dynamics. As the oceanic signal cannot be transmitted without time lag, we investigate meteorological features, which work on both the eastern North Atlantic and the North Sea concurrently. We find wind direction induced by large meteorological pressure patterns, responsible for the variability of the gyre dynamics and local shifts of water masses with strong horizontal gradients in the northern North Sea. In summary, salinity variations in the northern North Sea are governed by large-scale oceanic circulation, whereas winter nutrient variations are mainly driven by atmospheric variability.

1. Introduction

The North Sea is flushed mainly by North Atlantic water via its northern boundaries (Pätsch et al., 2017; Winther & Johannessen, 2006). The nutrient loads of this North Atlantic water have a large biogeochemical impact on the northern and central North Sea (Leterme et al., 2008). One example is the strength of the uptake of anthropogenic CO_2 from the atmosphere: The northern and central North Sea is observed to be a net sink of atmospheric CO_2 (Huthnance et al., 2009; Meyer et al., 2018; Thomas et al., 2004). There, primary production is the most important process lowering near-surface dissolved inorganic carbon and thus enhancing the uptake of atmospheric CO_2. Unlike the southern and coastal areas, primary production in the northern and central part of the North Sea is limited by the nutrients nitrate and phosphate

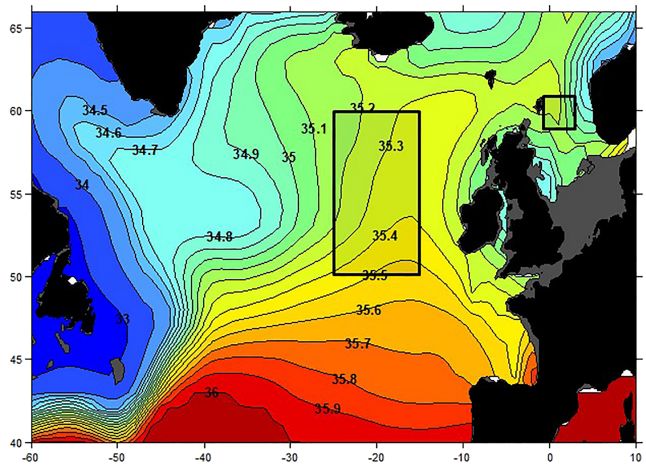

Figure 1. Mean salinity distribution at 66 m depth derived from the EN4 data set. The North Atlantic region (50–60°N, 25°W to 15°W) and the *Shetland region* (59–61°N, 1°W to 3°E) are indicated by black boxes.

(Holt et al., 2016). The diatom spring bloom in the North Sea and the adjacent North Atlantic is strongly limited by silicate concentrations (Allen et al., 2005; Henson et al., 2006). Besides local processes like stratification and vertical mixing, winter concentrations of these nutrients quantitatively govern annual primary production in the northern and central North Sea (Pätsch & Kühn, 2008). Thus, understanding the mechanisms driving the variability of winter nutrient concentrations in the northern and central North Sea is crucial for describing the variability of the most important biogeochemical processes in this area.

One possible candidate as mechanism behind the nutrient variability in the northern North Sea is the shift of water masses within the eastern North Atlantic, which governs the salinity variations in the northern North Sea in the following way: Salinity in the eastern subpolar North Atlantic (ENA) has repeatedly been shown to be related to the size and strength of the Subpolar Gyre (SPG) (Bersch, 2002; Häkkinen et al., 2011; Hátún et al., 2005; Sarafanov et al., 2018). When the SPG is weak, isopycnals in the subpolar North Atlantic relax, the Subpolar Front (SPF) in the ENA shifts westward, and the throughput of subtropical waters increases in the ENA. Model simulations show that the influence of the SPG variations extends to the northern North Sea as central part of the Northwest European Shelf Sea (Koul et al., 2019) (Figure 1).

Another candidate is the North Atlantic Oscillation (NAO), the dominant atmospheric mode over the North Atlantic. Hjøllo et al. (2009) found strong variability in volume fluxes in the northern North Sea driven by the NAO. Huthnance et al. (2016) found strongly elevated inflow from the North Atlantic into the North Sea for all inflow sections within the first half of the year after a high NAO winter index. The NAO also determines variations in wind fields. Mathis et al. (2015) studied westerly and southwesterly wind anomalies which resulted in changes in the water inflow patterns at the northern boundary of the North Sea. Schrum and Siegismund (2001) studied the time interval 1958–1997. They found a shift of more southerly winds toward west-southwesterlies in their last decade. This was accompanied by an enhancement of wind speed, which, in turn, increases the import of North Atlantic water into the North Sea across its northern boundary (Skogen et al., 2011). These examples show that the NAO variations impact wind speed and direction and thus the exchange of water masses between the North Atlantic and the North Sea.

Unlike the mechanism driving the interannual to decadal variability of salinity in the northern North Sea induced by advected North Atlantic water masses (Koul et al., 2019; Núñez-Riboni & Akimova, 2017), the controlling factors of nutrient concentrations are much more entangled, and nutrient concentrations in the northern North Sea and in the adjacent North Atlantic exhibit strong lateral gradients (Figure 2). Even though an earlier database (Radach & Pätsch, 1997) showed these gradients in northern winter concentrations, the southern North Sea dominated the discussion (Brockmann et al., 1988). Huthnance et al. (2009) characterized the seasonal to interannual variability of cross shelf-edge transport as due to changing properties of water flowing along the slope and other mechanisms. These findings were confirmed by model studies by Holt et al. (2012), who found that primary production in the North Sea depends on on-shelf fluxes of nitrate from the North Atlantic. Along the advective pathway from the North Atlantic into the North Sea, nutrients undergo seasonal variations because of processes like export production, remineralization, and vertical mixing. Also, the deep winter convection in the North Atlantic likely plays an important role for the fate of nutrients (Oschlies, 2002). Thus, it is unclear whether a nutrient signal in one year advected from the North Atlantic can be detected in the following year. To the best of our knowledge, no observational study has assessed the interannual to decadal variability in winter nutrient concentrations in the northern North Sea.

In this paper, we analyze the interannual and decadal variability of the macronutrients nitrate and phosphate as well as salinity in the northern North Sea. Silicate concentrations does not exhibit correlations as nitrate and phosphate do. For the sake of completeness the analysis of silicate concentrations is put into the supporting information (S1–S3). The basis of this analysis is a newly established biogeochemical

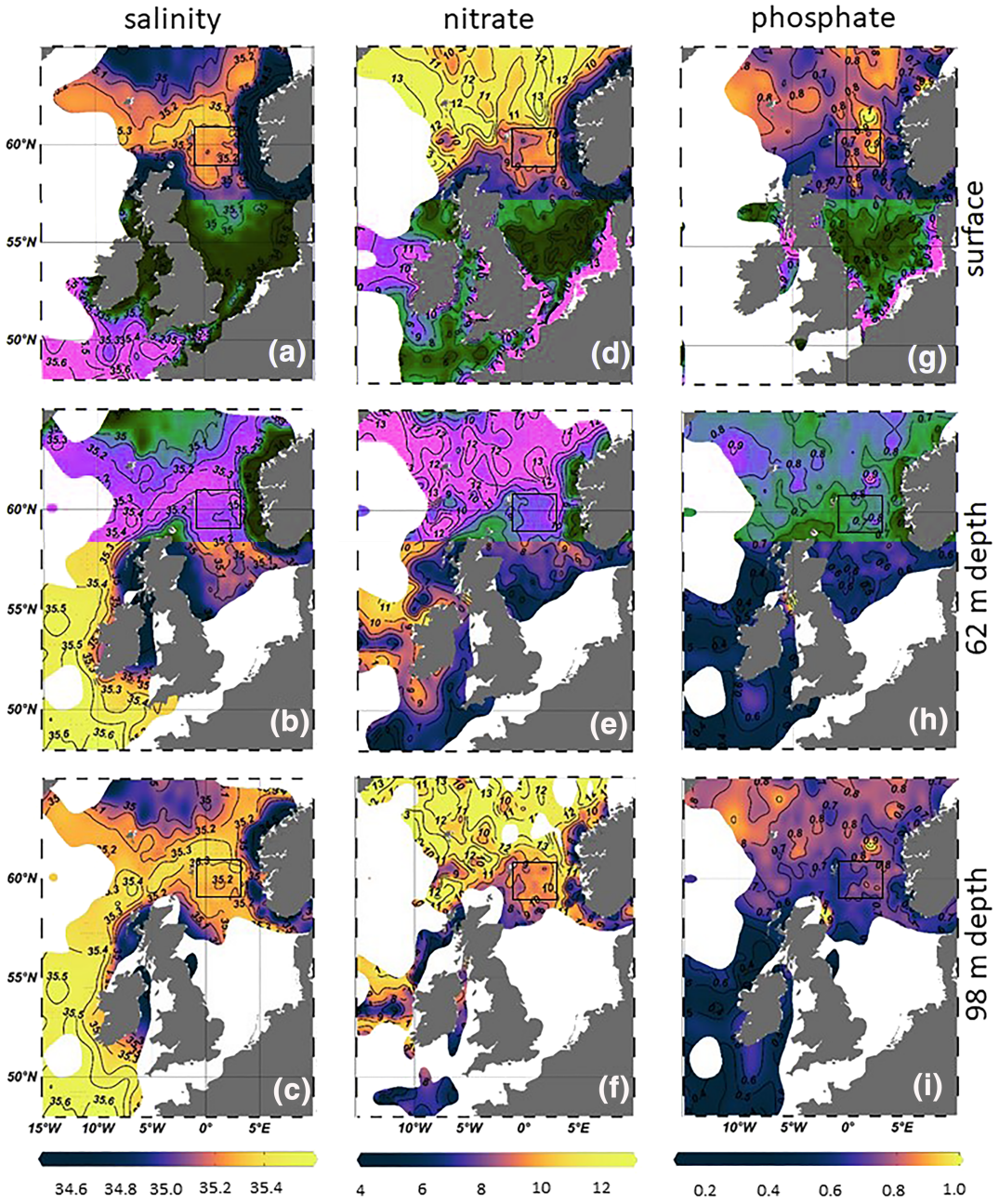

Figure 2. Mean horizontal winter (DJF) distribution of salinity (a–c), nitrate (mmol N-NO_3 m^{-3}) (d–f), and phosphate (mmol P-PO_4 m^{-3}) (g–i) at the surface (a–g) at 62 m (b, e, h) and 98 m depths (c, f, i) for the years 1984–2014. White areas indicate areas with water depth lower than the specific depth level or areas with very low data density. The *Shetland region* (1°W to 3°E, 59°N to 61°N) indicates the area in the northern North Sea where NSBC data were resolved temporally. The data are based on the Biogeochemical North Sea Climatology (NSBC).

North Sea Climatology (Hinrichs et al., 2017), which allows to discriminate depth resolved monthly mean concentrations on a (1/4)° × (1/4)° horizontal grid for each of the years 1960–2014.

Data handling, aggregation, and the building of consistent time series of annual winter concentrations of salinity, nitrate, and phosphate are described in section 2. In section 3 the results of the interannual to decadal analysis are presented. The findings are discussed and explained in section 4.

2. Methods

2.1. The North Sea Biogeochemical Climatology

By bringing together observations available from various data centers, a Biogeochemical North Sea Climatology (NSBC) has been constructed providing a suite of biogeochemical parameters for the wider North Sea region (48–65°N, 15°W to 15°E) for the time period 1960–2014. The parameters are nitrate, phosphate, silicate, ammonium, dissolved oxygen, and chlorophyll a. If available, these biogeochemical parameters are accompanied by temperature and/or salinity observations. For this paper only salinity, nitrate, and phosphate are used. Silicate has undergone the same analysis. The results are shown in the supporting information (S1–S3).

During the preparation of the climatology, a standardization of the observations was applied to the individual data sets to harmonize data formats and physical units of the parameters. Duplicates were removed, and a quality control procedure eliminated erroneous observations (Gouretski, 2018). A detailed report on the preparation of the Biogeochemical Climatology is given by Hinrichs et al. (2017).

The quality controlled profiles were interpolated on a set of unevenly spaced standard levels, using the weighted-parabola method (Reiniger & Ross, 1968). The vertical spacing is 5 m between the surface and 35, 42, and, 50 m, increasing linearly downward.

The quality-controlled profile data were averaged at each standard level within the $(1/4)° \times (1/4)°$ LAT/LON grid for each month. In case no data fall into a 3-D cell for a specific month, this cell gets a fail value for this month; otherwise the average, standard deviation, and the number of observations is assigned to the cell and month. After 1984, the data density strongly increases. This is the reason that the following analysis starts with the year 1984.

For the depth levels 0, 62, and 98 m it was possible to build climatological horizontal winter (December, January, February (DJF)) distributions of salinity, nitrate, and phosphate for the years 1984–2014 (Figure 2). For some areas, the data density was too low or the water depth was smaller than the depth level; these areas are left white. The *Shetland region* data, within the black rectangle, show only minor variations regarding the different vertical layers.

2.2. Data Aggregation

The *Shetland region* (59–61°N, 1°W to 3°E) represents the area in the northern North Sea where a strong inflow of water and nutrients from the North Atlantic occurs (Laane et al., 1996; Smith et al., 1996) (Figure 1). The more western inflow via the Fair Isle Current is weaker, and the water has to pass a relatively shallow bedrock sill, before entering the North Sea. Thus, the analysis concentrates on the Shetland inflow situated between the Fair Isle Current and the Norwegian Trench. Due to the important role of this inflow area, the winter nutrient concentrations within the *Shetland region* determine biogeochemical settings for large parts of the central and northern North Sea (Thomas et al., 2010).

The *Shetland region* contains 128 $(1/4)° \times (1/4)°$ cells. For each winter (DJF) the number of cells which are occupied by concentration values is counted. From 1984 to 2000, about 10% coverage is reached for the three parameters salinity, nitrate, and phosphate. After 2000, the coverages of the *Shetland region* for individual winters vary, but all winters are occupied by data. To check whether local biases were introduced, the average latitudinal and longitudinal positions of the corresponding observations were calculated for each winter. The mean latitudinal positions are for salinity always between 59.5°N and 60°N, and the longitudinal mean positions are found in the interval 0.4°W to 1.6°E. Nutrient mean positions fall in a bit wider range: Nitrate is in (59.4–60.2°N; 0.8°W to 1.2°E), and phosphate fall in (59.4–60.4°N; 0.4°W to 1.6°E). The complete coverage would have resulted in the mean position 60°N, 1°E).

To avoid clustering and biasing, winter (DJF) salinity, nitrate, and phosphate concentrations of the gridded NSBC data which are positioned within the *Shetland region* are vertically and temporally averaged (0–98 m and 3 months). In this way for some of the 128 $(1/4)° \times (1/4)°$ cells annual winter averages are built. Most of the cells are still not covered. To improve the data coverage for each year, the cells are aggregated into 16 larger $1° (\Delta\lambda) \times (1/2)° (\Delta\phi)$ cells. The rate of coverage over the *Shetland region* and over the years (DJF) becomes 63%, 56%, and 63% for salinity, nitrate, and phosphate, respectively. Four of the 16 cells entirely

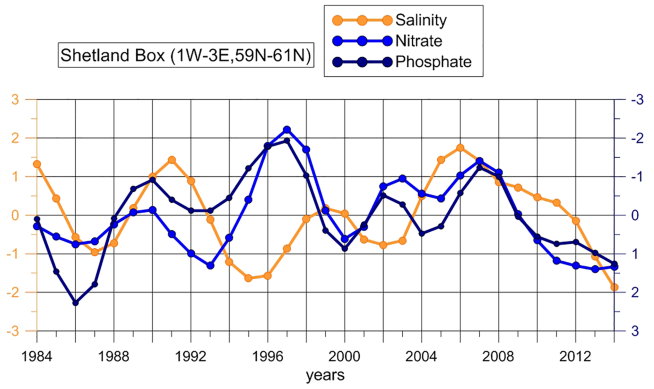

Figure 3. Mean winter salinities and nutrient concentration indices (DJF) within the *Shetland region*. The original data are averaged over the 98 m depth range. Note the reversed *y* axis for nitrate and phosphate.

cover the time interval 1984–2014 with the exception of one cell with one year missing. This single gap was filled by linear interpolation.

In order to build sound winter averages for the entire *Shetland region*, the gradients within this region (Figure 2) are taken into account. This implies that the winter averages are calculated from representative cell means, which means a full coverage of all cells for each winter. To fill the remaining gaps of the last 12 cells, correlations between already fully covered cells and incomplete cells are established and afterward used to fill the incomplete cells. To control this procedure, the newly filled time series of the cells are compared with time series for these cells, which are completely derived from the correlations even when the cells are already filled for specific years. In all cases the existing winter values are nearly reproduced.

The 16 complete time series of winter means of the filled series are averaged year by year resulting in annual winter concentration indices representative for the *Shetland region* (Figure 3). The transition from concentration values to concentration indices is explained in section 2.6.

2.3. Determination of the Mean Wind Direction

For the calculation of mean winter (DJF) wind direction within a defined area, the 6-hourly NCEP parameters uwnd and vwnd are used. They represent the zonal and meridional wind speed components 10 m above ground (Kalnay et al., 1996). For each pair of the wind components the meteorological wind direction (west wind $\triangleq$ 270°) is calculated. All wind directions within the defined area are spatially averaged. The mean winter wind direction is then calculated by averaging the spatial mean wind directions temporally.

2.4. The EN4 Data Set

We use annual mean salinity at 66 m depth from the EN4 data set (Good et al., 2013) within the ENA (50–60°N, 25–15°W) (Figure 1). It has been shown that the 66 m depth level is representative for the water column of the upper 98 m. This region has been chosen as it exhibits distinct zonal salinity gradients. Highest salinity values can be seen in the eastern part of this area, and lower values appear in the western part. A zonal displacement of the water mass in the eastern North Atlantic can be detected by the averaged salinity values in the indicated ENA region.

2.5. The SPF Index and the SPG Index

The position of the SPF is defined as the maximum longitude of the ~35.05 psu isohaline at 55°N and 100 m depth. This index captures the variability associated with the eastward (northward) extent of subpolar (subtropical) water in the ENA. Additionally, we define the SPG index as the principal component of the second mode of sea surface height variability in the North Atlantic (70°N, 80°W), as suggested by Hátún and Chafik (2018). The SPG index is available from 1993 onward (Figure 4).

2.6. Treatment of the Time Series

All time series are smoothed by applying a 3 year running mean. Additionally, all time series, but the time series of wind direction, are detrended and normalized. The normalization unifies the amplitudes by dividing the values by the standard deviation of the corresponding series. The corresponding dimensionless values are called indices. All correlations cited are significant ($p > 0.99$). The unworked winter averages are shown in supporting information S7.

3. Results

After the observational data were aggregated as described above, it was possible to fill the time series of all three parameters salinity, nitrate, and phosphate in the *Shetland region* for all years with winter values (Figure 3). The time series of salinity exhibits distinct decadal variabilities with local minima (including possibly the first and last years) around 1987, 1995, 2002, and 2014. Local maxima emerge around 1991, 1999, and 2006. The period of long-lasting descending values from 2004 to 2013 is characteristic. We tested the validity of the salinity time series and found that corresponding EN4 salinity winter means near the

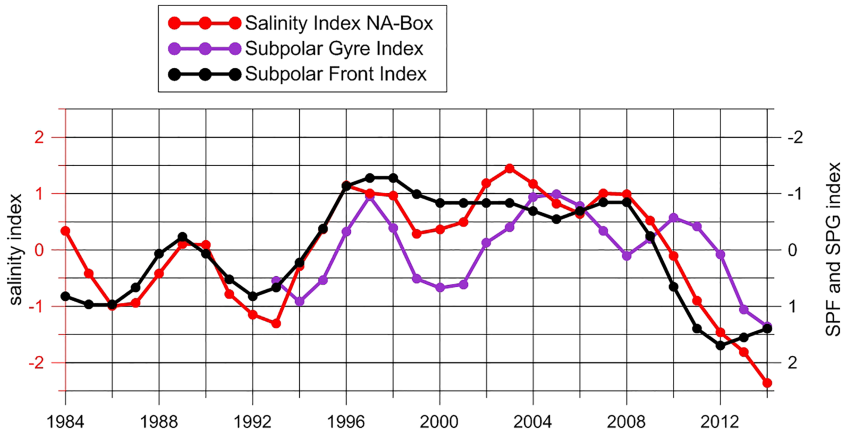

Figure 4. Relationship between the position of subpolar front, the subpolar gyre index, and the salinity index in the eastern subpolar North Atlantic.

Shetland region show very similar features (not shown). Due to the absence of biological activities, winter nutrient concentrations behave more or less conservative. They also show decadal variations, and the oscillations appear similar to those of salinity, but the local minima and maxima are phase shifted.

The observed variability in salinity is most likely due to the variability in the strength of the SPG. This is suggested by the relationship between the position of SPF, the SPG Index, and the salinity in the North Atlantic Box (Figure 4). When the SPG circulation is strong, the SPG shifts eastward, and the subpolar water masses dominate this region. This results in anomalous freshening of the ENA (Hátún et al., 2005; Koul et al., 2019). When the SPG is weak, the SPF shifts westward, and this region is dominated by subtropical water masses which lead to an increase in salinity.

To understand the mechanism driving the temporal variability of salinity in the northern North Sea, we compare it with data from the subpolar North Atlantic. Mean winter salinity in the *Shetland region* and annual mean salinity in the ENA compare well and show maximum correlation ($r = 0.66$) when the North Atlantic values are shifted by 2 years forward in time (Figure 5). A 3 year shift results in a less correlation ($r = 0.58$). In the same way, we compare the temporal variability of northern North Sea nutrient data with salinity data in the subpolar North Atlantic and find a striking similarity between the time series of salinity in the ENA and nitrate in the *Shetland region* (Figure 6). The correlation coefficient is $r = -0.87$ without a time shift. The absolute value of the coefficient decreases for all time shifts applied. This means that a westward shift of the water mass within the ENA (increase of salinity) coincides with low nitrate concentrations in the *Shetland region* and vice versa. Phosphate concentrations show a similar covariance with salinity in the ENA (Figure 6b). The correlation coefficient is $r = -0.61$. These statistical analyses are significant ($p > 0.99$) with sufficient annual data. The number of available nutrient observations in the *Shetland region* is at least 70 per winter (lower panels in Figure 6 and 6b).

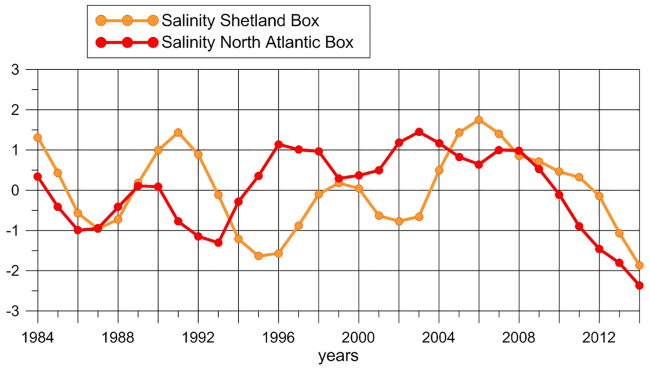

Figure 5. Annual mean salinity indices in the eastern subpolar North Atlantic (red line, 66 m depth level) and mean winter salinities in the *Shetland region* (orange line, 98 m depth average).

The time lag between salinities in the North Atlantic and the *Shetland region* suggests that the signal of high saline subtropical water caused by the westward shift of water mass in the ENA moves northward and appears in the *Shetland region* after 2 years. The mean concentrations of the near-surface nitrate south of Ireland, near 49°N, are lower than those at 60°N north of Ireland (Figures 2d and 2g). In case of advective nutrient signal transmission, this would explain the negative correlation between salinity in the ENA and nitrate in the *Shetland region*. However, the absolute value of the negative correlation is highest without any time lag. This is a mismatch with the findings regarding the connection between salinity in the ENA and salinity in the *Shetland region* with time lag of 2 years. This requires that other processes influencing the nutrient concentrations play a role. Candidates are other remote or local processes as well as processes

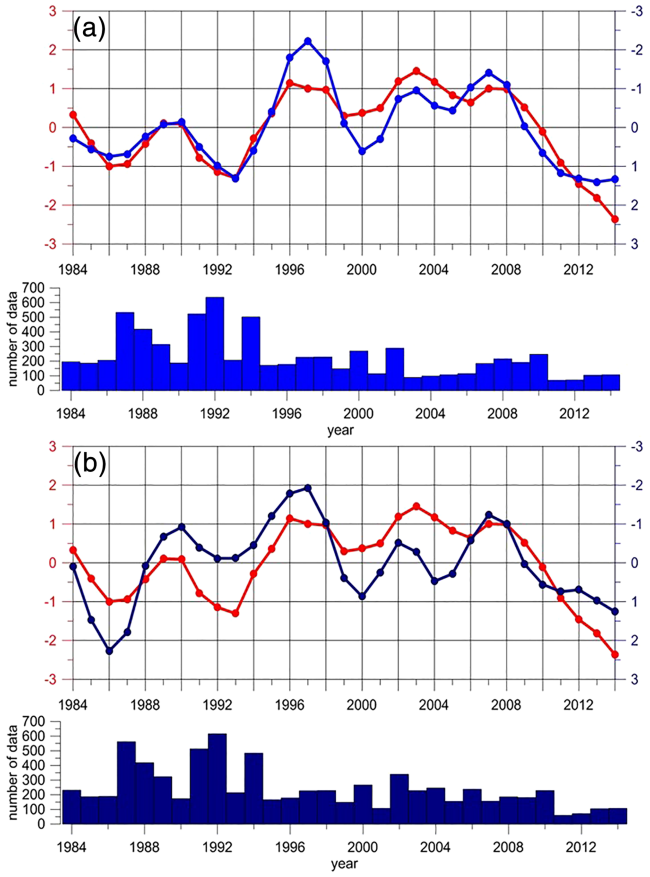

Figure 6. (a) Annual mean salinity indices in the eastern subpolar North Atlantic (red line, 66 m depth level) and mean winter nitrate concentration indices in the *Shetland region* (blue line, 98 m depth average). In addition, the number of underlying data for each winter is shown. (b) Mean annual salinity indices in the eastern subpolar North Atlantic (red line) and mean winter phosphate concentration indices in the *Shetland region* (dark blue line). In addition, the number of underlying data for each winter is shown.

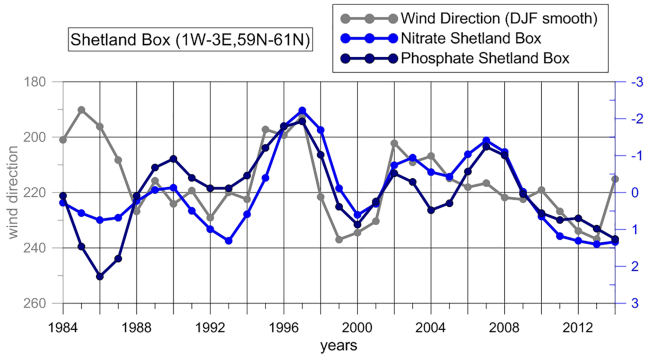

Figure 7. Mean winter wind direction within the *Shetland region* together with the mean winter concentration indices of the nutrients phosphate and nitrate (98 m depth average). Note the reversed *y* axes.

regarding lateral or vertical dynamics. As other remote processes would imply time lags too, and the vertical profiles of nitrate and phosphate appear homogeneous (Figure 2) over wintertime, only local lateral processes are left over to explain the variability of nitrate and phosphate in the Shetland region.

The absence of a time lag between salinity variations in the ENA and nutrient variations in the *Shetland region* does not suggest far-field oceanic variability as the causal mechanism. Nutrient concentrations within the *Shetland region* show strong horizontal gradients (Figures 2d and 2g). In addition, elevated nutrient concentrations can be observed northwest of the *Shetland region*, and lower concentrations appear in southwest direction. The elevated northwestern values are part of a large subpolar area with high nutrient concentrations. Thus, a southeastward or northwestward shift of the water within and around this region would change the mean nutrient concentration within the region immediately. Candidates for driving such water mass shifts are the wind strength, the wind stress curl, and the wind direction. Only for the wind direction significant correlations with the nutrient time series exist. Figure 7 shows the mean winter wind direction within the *Shetland region* together with the mean winter concentration indices of the nutrients phosphate and nitrate. From 1988 to 2014, wind direction and nitrate concentration indices correlate ($r = 0.63$). And, indeed, higher nitrate concentrations coincide with more westerly winds, whereas lower nitrate concentrations agree with more southern winds. The phosphate time series (1988–2014) correlates also with the wind direction ($r = 0.63$). The early years 1984–1987 do not show the coincidence of southern wind direction and lower indices. During this time, southern winds correspond with elevated nutrient conditions.orting information S5 shows the time series including wind speed and wind stress curl which are less correlated with nitrate and phosphate values. The atmospheric data for supporting information S5 are derived from a large field within the North Atlantic. From this figure it can be seen that the average wind speed is between 8.4 and 11 m/s. This means that the corresponding wind stress together with the wind direction forces the displacement of the water body in the *Shetland region*. Figure S8 of the supporting information also shows that there is no apparent influence of wind stress curl (S8a and S8b) and wind speed (S8e and S8f) on near-surface nitrate concentrations. Due to the lack of data, the relation between wind direction and near-surface nitrate distribution is not clearly visible (S8c and S8d).

The *Shetland region* represents that area of the northern North Sea where a strong inflow from the North Atlantic occurs. Therefore, one would expect a strong influence of winter nutrient variability in the *Shetland region* on nutrients in other parts of the North Sea. Figure 8 shows the winter surface distributions of salinity and the nutrients nitrate and phosphate for years with low (Figures 8a, 8c, and 8e) and high (Figures 8b, 8d, and 8f) winter nutrient concentrations in the *Shetland region* (cf. Figure 7). Two features discriminate these two situations: South of the *Shetland region*, the nutrient concentrations of the low winter situations are lower than those in the high winter situations. This affects large parts of the central North Sea. Even the local minimum at 55°N appears more extended in the low winter situations. This effect cannot be detected for salinity (Figures 8a and 8b). For salinity south of the *Shetland region* a local maximum appears (Figure 8a) which can be compared with elevated silicate values southwest of the *Shetland region* (Figure S3a).

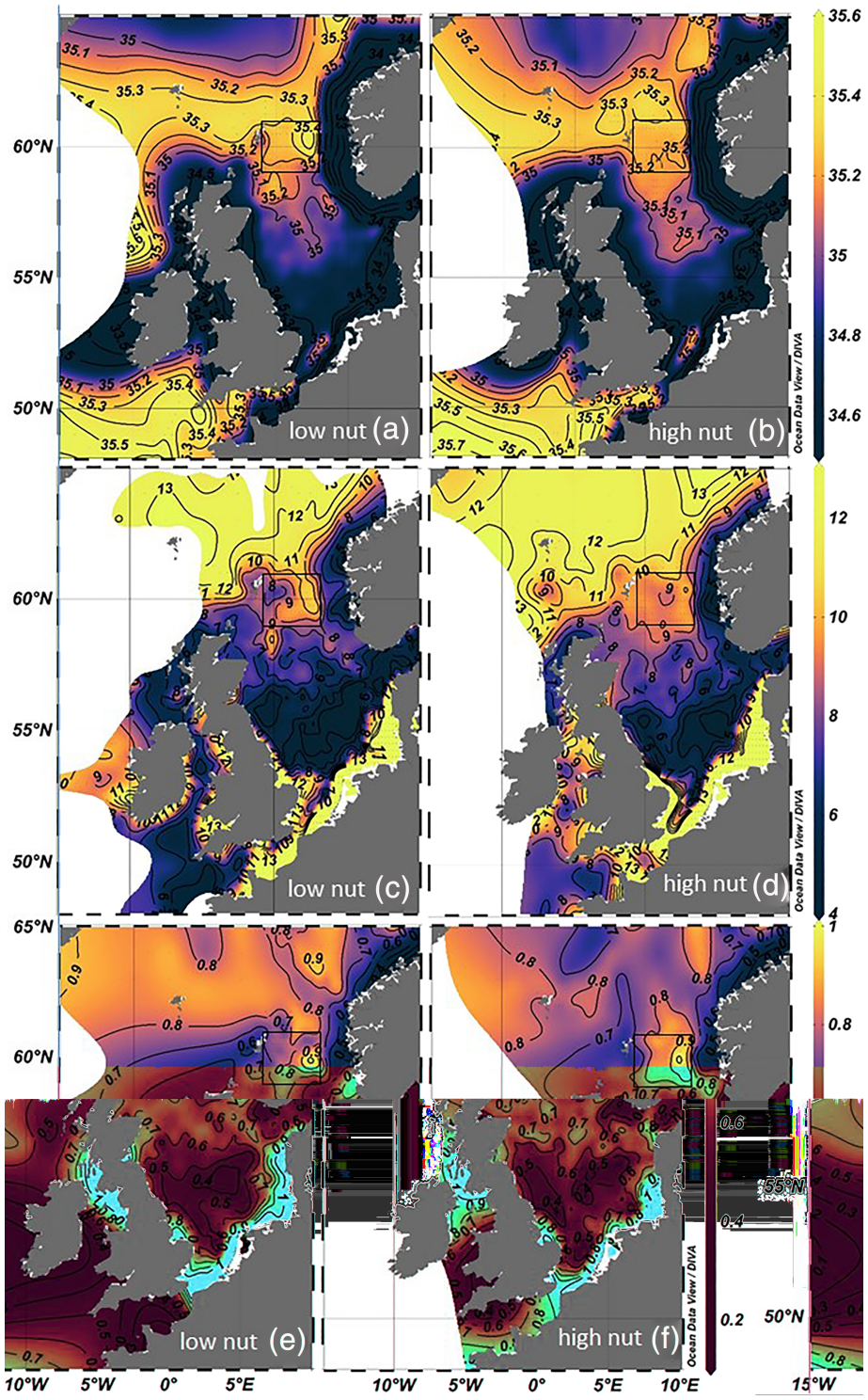

Figure 8. Mean horizontal winter (DJF) distribution of salinity (a, b), nitrate (mmol N-NO_3 m^{-3}) (c, d), and phosphate (mmol P-PO_4 m^{-3}) (e, f) at the surface. The left-hand side figures (a, c, e) depict years with low nutrient values in the *Shetland region* (1987, 1988, 1989, 1996, 1997, 1998, 2006, 2007, and 2008). The right-hand side figures (b, d, f) depict years with high nutrient values in the *Shetland region* (1985, 1986, 1987, 1992, 1993, 1994, 1999, 2000, and 2001).

4. Discussion

We present a novel observational study assessing the interannual to decadal variability in winter nutrient concentrations in the northern North Sea. Based on simulation results, the correlation between salinity in the eastern North Atlantic and the northern North Sea has been subject of several assessments. Koul et al. (2019) and Núñez-Riboni and Akimova (2017) found an advective lag of about 1 year between the Rockall Trough (near 12°W, 57°N) and the North Sea entrance. As Rockall Trough is about half the way to the center of the ENA defined in the present study, the 2 year time lag derived from NSBC and EN4 data appears reasonable. This is also supported by the analysis of the correlation between salinity in the ENA and the *Shetland region* derived only from EN4 yielding a time lag of 2 years as well. The conclusion of this analysis might be weakened as the underlying observations of the EN4 and the NSBC data set might overlap. A deeper analysis of the annual mean salinity anomalies of the upper 98 m within the EN4 data on a section from the center of the North Atlantic region (0 km) to the center of the *Shetland region* (1650 km) reveals also mean propagation time of salinity signals of 2 years (supporting information S4). A further confirmation of these results is given by a TS-diagram of annual mean depth-averaged temperature and salinity EN4 values taken from the North Atlantic Box and from the *Shetland region* (supporting information S9). The two water bodies are positioned on nearly the same isopycnal.

It appears that the mechanism, which drives salinity variations in the northern North Sea, cannot be translated directly into nutrient dynamics. Of course, the water masses, which are transported over years from the subtropical North Atlantic toward the northern North Sea, carry also the signal of low nutrient concentrations, but the biologically induced annual cycle masks this signal. Consequently, we could not detect this advected signal in nutrients.

The westward shift of the SPF is often attributed to a decrease in westerly winds (in favor of more southerly winds) (Bersch et al., 2007; Hátún et al., 2005). Due to the similarity of wind directions over the northern North Sea and the eastern North Atlantic, an increase of salinity in the ENA is correlated with lower nutrient concentrations in the *Shetland region*. So the explanation for the anticorrelation between salinity in the ENA and nutrient concentrations in the *Shetland region* is due to the large-scale meteorological fields over the north-eastern North Atlantic.

Contrasting situations with low and high winter nutrient concentrations in the *Shetland regio*n allow further insights into the dynamics of winter nutrients there. Within the *Shetland region*, the zonal gradient of all three parameters salinity, nitrate, and phosphate is higher during low winter nutrient situations than during high winter concentrations. In low winter nutrient situations, relatively high values can be detected in the eastern part of the region close to the western flank of the Norwegian Trench. The source of these local maxima might be attributed additionally to the fact that water near the eastern edge of the *Shetland region* is no longer shifted eastward by westerly winds, and thus, water masses from the Norwegian Trench have larger influence.

To check the consequences of winter nutrient variability, we investigate anomalies of chlorophyll a concentrations in the northern and central North Sea (supporting information S6). Due to the rareness of chlorophyll a observations, we found large parts of months unfilled. A hint of a relation between the elevation of winter nutrient concentrations and subsequent chlorophyll a concentration was found for April 1990 and 1996 with low chlorophyll a concentrations corresponding with low nitrate and phosphate concentrations in these years (Figure 3).

5. Conclusion and Outlook

This study represents the first observational data-based attempt to explain the interannual winter nutrient concentration along the European margin. It shows that interannual to decadal variations of salinity in the northern North Sea are governed by the SPG variability in the ENA. This signal, mediated by advection of North Atlantic water masses, reaches the North Sea with a time lag of 2 years. As low nitrate and phosphate concentrations of the subtropical North Atlantic can be differentiated from high nitrate and phosphate concentrations in the subpolar North Atlantic, one would expect to find a similar mechanism for nitrate and phosphate as for salinity. Since we have not found these signals for nitrate and phosphate, we conclude that nitrate and phosphate concentrations in the northern North Sea are

not governed by water mass variations originating in the North Atlantic. Instead, we found an interannual to decadal variability of nitrate and phosphate concentrations in the northern North Sea affected by regional (and large-scale) meteorological fields. As such a coincidence of silicate anomalies and variations of large-scale meteorological fields could not be detected, we conclude that the special lateral distribution of nitrate and phosphate concentrations is responsible for the detected correlations. The North Sea is as an example of a broad shelf sea with an open ocean far from the nutrient-enriched continental coast. It covers distinctly separated local maxima and minima of nutrient concentrations in the different regions.

In future related work we recommend to analyze larger regions allowing to study possible interactions between water mass and meteorological variations. Due to the lack of observational data, such work may be extended to model studies over even larger time spans.

Acknowledgments
This work was supported through the Cluster of Excellence CliSAP (EXC177), University of Hamburg, funded through the German Research Foundation (DFG). Vimal Koul's work is a contribution to the Climate, Climatic Change, and Society (CliCCS) project A5. We thank M. Bersch, three anonymous reviewers, and the biogeochemical experts U. Brockmann, H. Thomas, K. Emeis, and H. -J. Lenhart for valuable discussions. The NSBC data are deposited in the ICDC database https://icdc.cen.uni-hamburg.de/daten/ocean/nsbc/ and the EN4 data are deposited online (https://www.metoffice.gov.uk/hadobs/en4/download-en4-2-1.html). The annual mean SSH data (i.e., AVISO absolute dynamic topography on a 0.25° × 0.25° grid) to calculate the SPG index were obtained from the Integrated Climate Data Center (http://icdc.cen.uni-hamburg.de/1/daten/ocean/ssh-aviso.html).

References

Allen, J. T., Brown, L., Sanders, R., Mark, M. C., Mustard, A., Fielding, S., et al. (2005). Diatom carbon export enhanced by silicate upwelling in the northeast Atlantic. *Nature*, *437*(7059), 728–732. https://doi.org/10.1038/nature03948

Bersch, M. (2002). North Atlantic Oscillation-induced changes of the upper layer circulation in the northern North Atlantic Ocean. *Journal of Geophysical Research*, *107*(C10), 3156. https://doi.org/10.1029/2001JC000901

Bersch, M., Yashayaev, I., & Koltermann, K. P. (2007). Recent changes of the thermohaline circulation in the subpolar North Atlantic. *Ocean Dynamics*, *57*, 223–235. https://doi.org/10.1007/s10236-007-0104-7

Brockmann, U., Salomons, W., Bayne, B. L., Duursma, E. K., & Foerstner, U. (1988). North Sea nutrients and eutrophication. In W. Salomons, B. L. Bayne, E. K. Duursma, & U. Foerstner (Eds.), *Pollution of the North Sea* (pp. 348–389). Berlin Heidelberg: Springer Verlag.

Good, S. A., Martin, M. J., & Rayner, N. A. (2013). EN4: Quality controlled ocean temperature and salinity profiles and monthly objective analyses with uncertainty estimates. *Journal of Geophysical Research, Oceans*, *118*, 6704–6716. https://doi.org/10.1002/2013JC009067

Gouretski, V. (2018). World ocean circulation experiment—Argo global hydrographic climatology. *Ocean Science*, *14*, 1127–1146. https://doi.org/10.5194/os-14-1127-2018

Häkkinen, S., Rhines, P. B., & Worthen, D. L. (2011). Warm and saline events embedded in the meridional circulation of the northern North Atlantic. *Journal of Geophysical Research*, *116*, C03006. https://doi.org/10.1029/2010JC006275

Hátún, H., & Chafik, L. (2018). On the recent ambiguity of the North Atlantic subpolar gyre index. *Journal of Geophysical Research, Oceans*, *123*, 5072–5076. https://doi.org/10.1029/2018JC014101

Hátún, H., Sando, A. B., Drange, H., Hansen, B., & Valdimarsson, H. (2005). Influence of the Atlantic subpolar gyre on the thermohaline circulation. *Science*, *309*(5742), 1841–1844. https://doi.org/10.1126/science.1114777

Henson, S., Sanders, R., Holeten, C., & Allen, J. (2006). Timing of nutrient depletion, diatom dominance and a lower-boundary estimate of export production for Irminger Basin, North Atlantic. *Marine Ecology-Progress Series*, *313*, 73–84.

Hinrichs, I., Gouretski, V., Pätsch, J., Emeis, K.-C., Stammer, D., (2017). North Sea biogeochemical climatology (https://icdc.cen.uni--hamburg.de/daten/ocean/nsbc/). World data Center for Climate (WDCC) at DKRZ.

Hjøllo, S. S., Skogen, M. D., & Svendsen, E. (2009). Exploring currents and heat within the North Sea using a numerical model. *Journal of Marine Systems*, *78*(1), 180–192.

Holt, J., Butenschön, M., Wakelin, S. L., Artioli, Y., & Allen, J. I. (2012). Oceanic controls on the primary production of the northwest European continental shelf: Model experiments under recent past conditions and a potential future scenario. *Biogeosciences*, *9*(1), 97–117.

Holt, J., Schrum, C., Cannaby, H., Daewel, U., Allen, I., Artioli, Y., et al. (2016). Potential impacts of climate change on the primary production of regional seas: A comparative analysis of five European seas. *Progress in Oceanography*, *140*, 91–115.

Huthnance, J., Weisse, R., Wahl, T., Thomas, H., Pietrzak, J., Souza, A. J., et al. (2016). Recent change—North Sea. In M. Quante, & F. Colijn (Eds.), *North Sea region climate change assessment, regional climate studies* (pp. 85–136). Berlin Heidelberg: Springer. https://doi.org/10.1007/978-3-319-39745-0_3

Huthnance, J. M., Holt, J. T., & Wakelin, S. L. (2009). Deep ocean exchange with west-European shelf seas. *Ocean Science*, *5*(4), 621–634.

Kalnay, E., Kanamitsu, M., Kistler, R., Collins, W., Deaven, D., Gandin, L., et al. (1996). The NCEP/NCAR 40-year reanalysis project. *Bulletin of the American Meteorological Society*, *77*(3), 437–471.

Koul, V., Schrum, C., Düsterhus, A., & Baehr, J. (2019). Atlantic inflow to the North Sea modulated by the subpolar gyre in a historical simulation with MPI-ESM. *Journal of Geophysical Research, Oceans*, *124*, 1807–1826. https://doi.org/10.1029/2018JC014738

Laane, R., Svendsen, E., Radach, G., Groeneveveld, G., Damm, P., Pätsch, J., et al. (1996). Variability in fluxes of nutrients (N,P,Si) into the North Sea from the Atlantic Ocean and Skagerrak caused by variability in water flow. *DHZ*, *48*(3/4), 401–419.

Leterme, S., Pingree, R., Skogen, M., Seuront, L., Reid, P., & Attrill, M. (2008). Decadal fluctuations in North Atlantic water inflow in the North Sea between 1958-2003: Impacts on temperature and phytoplankton populations. *Oceanologia*, *50*, 59–72.

Mathis, M., Elizalde, A., Mikolajewicz, U., & Pohlmann, T. (2015). Variability patterns of the general circulation and sea water temperature in the North Sea. *Progress in Oceanography*, *135*, 91–112.

Meyer, M., Pätsch, J., Geyer, B., & Thomas, H. (2018). Revisiting the estimate of the North Sea air-sea flux of CO_2 in 2001/2002: The dominant role of different wind data products. *Journal of Geophysical Research Biogeosciences*, *123*(5), 1511–1525.

Núñez-Riboni, I., & Akimova, A. (2017). Quantifying the impact of the major driving mechanisms of inter-annual variability of salinity in the North Sea. *Progress in Oceanography*, *154*, 25–37.

Oschlies, A. (2002). Nutrient supply to the surface waters of the North Atlantic—A model study. *Journal of Geophysical Research*, *107*(C5), 3046. https://doi.org/10.1029/2000JC000275

Pätsch, J., Burchard, H., Dieterich, C., Gräwe, U., Gröger, M., Mathis, M., et al. (2017). An evaluation of the North Sea circulation in global and regional models relevant for ecosystem simulations. *Ocean Modelling*, *116*, 75–90.

Pätsch, J., & Kühn, W. (2008). Nitrogen and carbon cycling in the North Sea and exchange with the North Atlantic—A model study. Part I. Nitrogen budget and fluxes. *Continental Shelf Research*, *28*, 767–787.

Radach, G., & Pätsch, J. (1997). Climatological annual cycles of nutrients and chlorophyll in the North Sea. *Journal of Sea Research*, *38*, 231–248.

Reiniger, R. F., & Ross, C. K. (1968). A method of interpolation with application to oceanographic data. *Deep-Sea Research*, *15*, 185–193.

Sarafanov, A., Falina, A., Sokov, A., Zapotylko, V., & Gladyshev, S. (2018). Ship-based monitoring of the northern north Atlantic Ocean by the Shirshov Institute of Oceanology. The main results. In *The Ocean in Motion* (pp. 415–427). Cham: Springer.

Schrum, C., & Siegismund, F. (2001). Decadal changes in the wind forcing over the North Sea. *Climate Research*, *18*(1–2), 39–45.

Skogen, M. D., Drinkwater, K., Hjollo, S. S., & Schrum, C. (2011). North Sea sensitivity to atmospheric forcing. *Journal of Marine Systems*, *85*, 106–114.

Smith, J. A., Damm, P. E., Skogen, M. D., Flather, R. A., & Pätsch, J. (1996). An investigation into the variability of circulation and transport on the North-West European Shelf using three hydrodynamical models. *DHZ*, *48*(3/4), 325–347.

Thomas, H., Bozec, Y., De Baar, H., Elkalay, K., Frankignoulle, M., Kühn, W., et al. (2010). Carbon and nutrient budgets of the North Sea. In K. K. Liu, L. Atkinson, R. Quinones, & L. Talaue-McManus (Eds.), *Carbon and nutrient fluxes in global continental margins—A global synthesis*, (pp. 346–355). New York: springer.

Thomas, H., Bozec, Y., Elkalay, K., & De Baar, H. J. W. (2004). Enhanced open ocean storage of CO_2 from shelf sea pumping. *Science*, *304*(5673), 1005–1008. https://doi.org/10.1126/science.1095491

Winther, N. G., & Johannessen, J. A. (2006). North Sea circulation: Atlantic inflow and its destination. *Journal of Geophysical Research*, *111*, 12. https://doi.org/10.1029/2005JC003310